Short-Term Electromagnetic Interference on a Buried Gas Pipeline Caused by Critical Fault Events of a Wind Park: A Realistic Case Study

D. Chrysostomou, A. Dimitriou, N. Kokkinos and C. A. Charalambous, *Member, IEEE*

***Abstract* — Short-term Electromagnetic Interference (EMI) pertains to the total result produced by the occurrence of intermittent, inductive and conductive couplings on a buried pipeline system. For example, this type of EMI takes place when considering the fault conditions of a single a.c. power line, acting in the nearby vicinity of a pipeline system. In the context of this paper, the effect of the short-term EMI is unfolded through a real case study. This case study involves a 20.7 MW Wind Park with extended underground power cable connections, which are laid nearby a high-pressure gas pipeline system. In particular, the impact of critical fault events, associated with the Wind Park's power cables, on the pipeline system is comprehensively assessed. The assessment is achieved by the concurrent use of two powerful software tools that are respectively eligible for the accurate short-circuit analysis of the electrical circuit of the Wind Park and for EMI evaluation on the pipeline. To this extent, the simulation results are thoroughly discussed and an effective mitigation solution is evidently presented.**

***Index Terms* — Electromagnetic Interference, Wind Park, Conductive Coupling, Power Cables, Insulation Joints, Gas Pipelines.**

I. Introduction

SHORT-TERM Electromagnetic Interference (EMI) is the total effect produced, by the fault conditions of a power line, in an interfered pipeline system. If the pipeline system is buried below the earth surface, this total effect pertains to the intermittent but concurrent act of two coupling mechanisms, namely, the conductive and the inductive. To this end, quite a few international standards [1]-[4] dictate that these two mechanisms should be evaluated when considering the fault conditions of a single a.c. power line (acting solely) in the nearby vicinity of a pipeline system.

To stress the importance of considering both coupling mechanisms in short-term EMI evaluations, we note the following: a) With regard to the inductive coupling, it should be borne in mind that it is possible to have intense magnetic field caused by the large current which may flow in the faulted phase conductors. The strong magnetic field may force the coating stress voltage of a pipeline to reach extremely high levels - in areas where large collocation lengths exist. The latter can take place in remote areas that are distant to the actual fault location [5]-[7]. b) The conductive coupling is prominent in places where a large fault current is injected into the earth [8]. As a consequence the local soil potential is raised and a voltage gradient in ground is formed. Nonetheless, the pipeline's metal located near the fault injection point will normally remain at a relatively low potential. This is due to the high resistance of the pipeline's coating and its grounding scheme at multiple points along its routing. Thus, the combination of high earth voltage (immediately outside the pipeline's coating) and the low potential of the pipeline's metal, gives rise to high coating stress voltages. (Note: The coating stress voltage is defined as the voltage between the pipeline metal and the earth immediately outside the coating).

Therefore, the straightforward conclusion is that, unless the pipeline crosses the power line's routing at or near 90°, the pipeline will suffer from both inductive and conductive interference. The latter basically entails that in the event of faults - occurring in adjacent power lines – severe harmful voltages and severe coating stress voltages can build up on the pipeline. The high stress voltage may be the cause of localized coating defects or the cause for derating the dielectric strength of the pipelines' insulation flange kits [9]. To make this argument more explicit, we note that pipelines' insulation flange kits are typically rated at 1000 V while monolithic insulation joints at 5000 V and may be affected in the event of short term EMI, unless appropriate surge protection is installed [3]. As stated in [3], this is because, "*surge protection, across insulation flanges, installed to mitigate against lightning may not be appropriate for the control of appropriately rated fault currents on nearby power lines*".

Thus, the calculated coating stress voltage, under short-term EMI events, shall be assessed to determine whether it can affect the integrity of the pipeline or whether it violates any human-hazard limits. The extent and the type of calculations required, suggest that they can only realistically be undertaken with the aid of computers [5], [10], [11]. This endeavor however, necessitates specialist knowledge in the fields of pipelines' protection and in earthing/grounding practices. Most importantly, the specialists should have the ability to discern what parameters can be safely neglected or what parameters are necessary to accurately represent the EMI processes that occur in each case-study.

C. A. Charalambous, A. Demetriou and D. Chrysostomou are with the Department of Electrical and Computer Engineering, Faculty of Engineering, of the University of Cyprus, PO Box 20537, 1687, Nicosia, Cyprus (e-mail of corresponding author: cchara@ucy.ac.cy).

N. Kokkinos is with ELEMKO SA, 90 TATOIOU Metamorphosis, 144 52, Greece

A. Explicit Contributions beyond the State-of-the-Art

This paper manifests the quintessence of the above discussion through a real case study. The case study involves a 20.7 MW Wind Park with extended underground power cable connections, which are crossing or running in parallel with a high-pressure gas pipeline system. The explicit contributions of this paper are listed as follows:

1) Interfacing two Powerful Software Tools to improve the accuracy of the final EMI evaluation:

The main objective of the paper is to assess the impact of critical fault events - associated with the Wind Park's underground power cables - on the gas pipeline system. The assessment is achieved by the concurrent use of two software tools, namely DIgSILENT Power Factory [12] and CDEGS [13]. These software tools are respectively eligible for the accurate short-circuit analysis of the electrical circuit associated with the Wind Park's electrical topology and for a numerical EMI evaluation [14] - accounting for the geographically accurate routings of the pipeline and the power cables. We wish to highlight that the modelling endeavour presented in the paper responds to the pressing need of fully exploiting the complementary strengths and data exchange between different simulation tools. This is dictated in order to improve the accuracy of the final evaluation result. In particular the short-circuit analysis performed by DIgSILENT Power Factory is appropriately integrated into the EMI evaluation tools of the CDEGS software.

2) Comprehensive modelling of the short-term EMI principles by accounting for the underground power cables' operation, design and bonding configurations:

The short-term EMI calculation principles resulting from underground HV cables are slightly more complex than that of bare overhead transmission line conductors. The Canadian standard [2] explicitly marks the similarities and differences that arise when the EMI on buried pipelines is produced by overhead lines and underground cables respectively. However, the modelling of short-tern EMI from power cables is not fully covered in the scientific literature. Thus, the modelling endeavor in this paper fully accounts for: a) the layout of the power cable systems (e.g. bonding and grounding methods across cables' routings), b) the size and electrical/ material characteristics of the structural components of the power cables (e.g. core, insulation, sheath), c) the type and location fault with respect to the bonding points and d) the correct topology of the power cables' layout with respect to the pipeline routing. To this extent, the modelling features (a-d) ensure that the concurrent act of the inductive and conductive couplings on the pipeline is appropriately accounted for.

B. Organization of the Paper

Bearing the above remarks in mind, the paper is organized as follows: Section II firstly provides an overview of the physical system under study, as well as a detailed description of the two simulation models and their input parameters. Section III provides details on the simulation approach. In particular, it includes the accurate short-circuit analysis carried out on the Wind Park Model and the interface of this analysis to the EMI model to investigate the impact on the pipeline system. The produced EMI analysis is then thoroughly discussed and a mitigation solution is provided.

II. Description of Simulation Models

A. Description of Physical and Simulation Models

Figure 1 shows the layout of the physical system which has been considered in this case study. In particular, the geographical location of the Wind Turbines (WTs) with respect to the natural gas pipeline routing is displayed. The Wind Park includes nine WTs with total rated capacity of 20.7 MW with their associated interconnections and control.

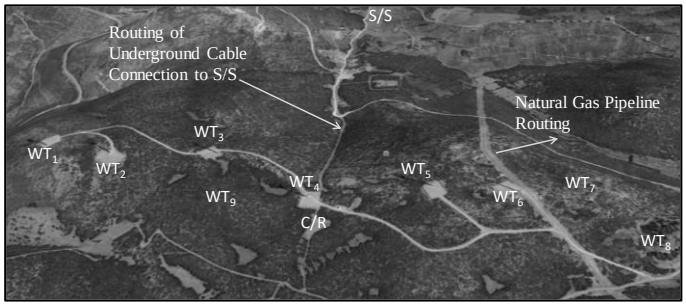

Fig. 1. Layout of the Physical System Under Study

B. Description of Electrical Circuit Model (DIgSILENT)

The electrical circuit associated with the WTs connections is shown in Fig. 2. This circuit is modelled in DIgSILENT Power Factory. In particular, the 9 WTs (2.3 MW each) are interconnected to a central control room (C/R), through underground cable connections. From the C/R, the power is transferred to an MV/HV substation (S/S) that is located 6.2 km away. The details of the cables' interconnections are given in Table I.

TABLE I
Characteristics of Underground Cable Connections

Cable Connection	Type of Cable	Formation	Circuit Length
WT_2-WT_1	20 kV XLPE 3×(1×240/25 mm^2)	Flat	372m
WT_1-WT_3	20 kV XLPE 3× (1×240/25 mm^2)	Flat	706m
WT_3-C/R	20 kV XLPE 3× (1×240/25 mm^2)	Flat	567m
WT_4-C/R	20 kV XLPE 3× (1×240/25 mm^2)	Flat	155m
WT_9-C/R	20 kV XLPE 3× (1×240/25 mm^2)	Flat	373m
WT_6-WT_5	20 kV XLPE 3× (1×240/25 mm^2)	Flat	686m
WT_5-C/R	20 kV XLPE 3× (1×240/25 mm^2)	Flat	771m
WT_8-WT_7	20 kV XLPE 3× (1×240/25 mm^2)	Flat	785m
WT_7-C/R	20 kV XLPE 3× (1×240/25 mm^2)	Flat	990m
C/R – S/S	20 kV XLPE 3× (1×630/35 mm^2)	Trefoil	6.2 km

More explicitly, the network model in Fig. 2 consists of 9 individual WTs, modeled as doubly-fed induction generators (DFIG). Each WT is supplying the corresponding 20 kV cable, via a step up transformer (0.69 kV /20 kV). Thus, the dashed rectangle in the inset detail of Fig. 2, illustrates this. This type of modeling represents a typical configuration of a wind farm, where each wind turbine is connected to a step-up transformer which boosts the generating output of the turbine generator. These transformers are typically small in MVA rating and they

are located at the base of the WT. From each WT, the power is interconnected through the main 6.2 km, 20 kV cable (C/R to the S/S) to a MV/HV step-up transformer at the substation (S/S), to be transported to the main HV grid.

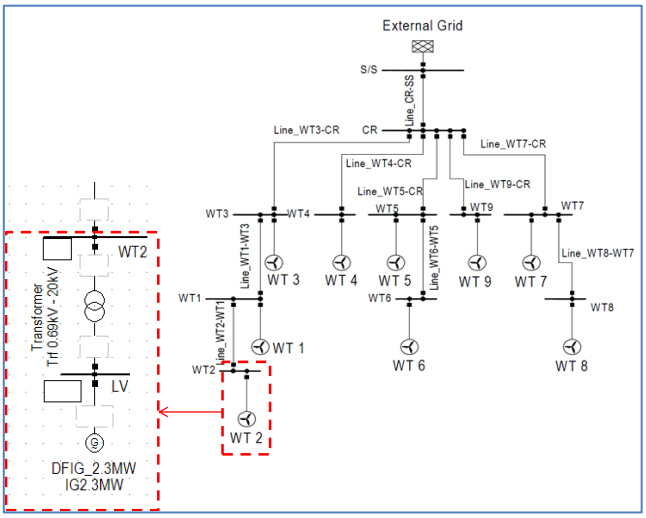

Fig. 2. Layout of the Electrical Circuit as Modeled in DIgSILENT Power Factory

C. *Description of EMI Model (CDEGS)*

The layout and the characteristics of the physical system shown in Fig.1 have been modelled in the CDEGS software [13]. This was achieved thorough the object-based graphical environment (SESCAD) that allows for the development of arbitrary networks of conductors to be arranged in such a way to reflect the true topology of the infrastructures and cables involved in the study.

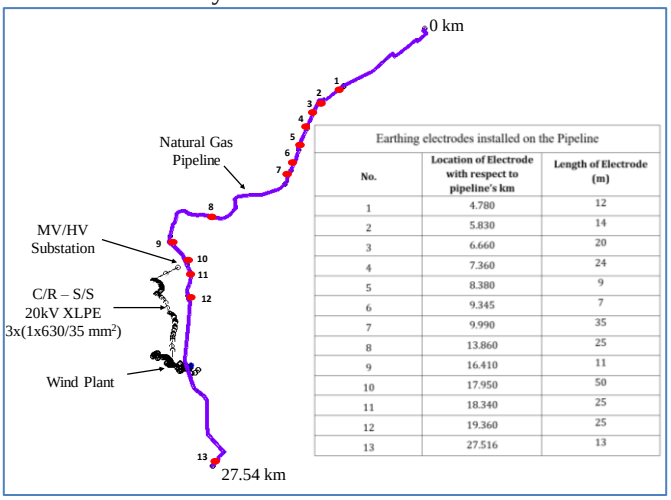

Fig. 3. Complete Layout of the EMI model within CDEGS

Thus, the developed model (see Fig.3) includes the gas pipeline as well the Wind Park's earthing systems and the associated MV power cables. Moreover, the model has accounted for the location (marked as 1-13 in Fig.3) and the design characteristics (embedded Table in Fig.3) of the earthing mitigation - electrodes that are currently installed on the gas pipeline within a 28km range.

To elucidate the details of the simulation model shown in Fig. 3, a portion of the computer model formulated - is illustrated in greater detail in Figures 4 and 5 respectively. To this end, Fig. 4 shows the design detail that corresponds to the Wind Park's topology with respect to the pipeline's routing. In particular, this zoomed figure illustrates the layout of the main power cables (3 x XLPE 630/35 mm^2) that are lead to the S/S. In addition, Fig. 4 illustrates the design detail of the earthing system associated with each WT. The earthing system has been modelled using equivalent cylindrical conductors. The characteristics (i.e. size and resistivity) of these conductors were calibrated to provide approximate the same resistance to earth value of each WT as measured in the field. A verification of this calibration process is provided in Table II.

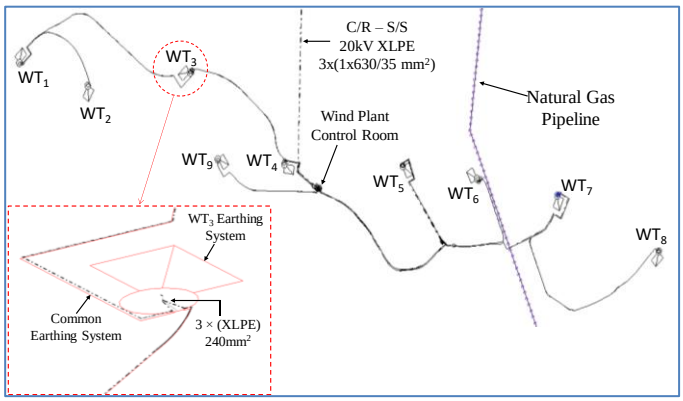

Fig. 4. Simulation Model Showing the Design Detail of the Wind Park's Cable Connections and WT's Earthing Systems

TABLE II
VERIFICATION OF MEASURED AND MODEL'S EARTH RESISTANCES FOR WTS AND CONTROL ROOM

	Measured Resistance to Earth (Ω)	CDEGS Calculated Resistance to Earth (Ω)
WT1	14.59	14.1
WT2	20.62	19.54
WT3	7.75	7.98
WT4	10.79	11.07
WT5	10.51	9.45
WT6	20.68	22.1
Control Room (C/R)	8.72	9.56

Moreover, Fig. 5 shows the design detail of some of the cables' (3 x XLPE 240/25 mm^2) routing and layout. These are the cables that are routed from the WTs to the control room (C/R). This figure also illustrates the cables' sheath bonding to a common earthing system (Cu -120mm^2) that spans across the Wind Park. The common earthing system reflects on the earthing practice that is regularly applied in Wind Parks. This practice pertains to interconnecting the earthing systems of each Wind Turbine, through earthing conductors (typically Cu having an equivalent cross sectional area of 120mm^2). The earthing/interconnecting conductors are usually placed in the same trench as the power cables. The most common practice, to this extent, is to place the earthing conductors below the power cables (Note: In Fig. 5 the earthing conductors are indicated with the red solid lines, while the power cables are indicated with dashed lines). The spacing between the earthing conductors and the power cables should be sufficient (e.g. 30-50cm) to allow for the efficient performance of the earthing system.

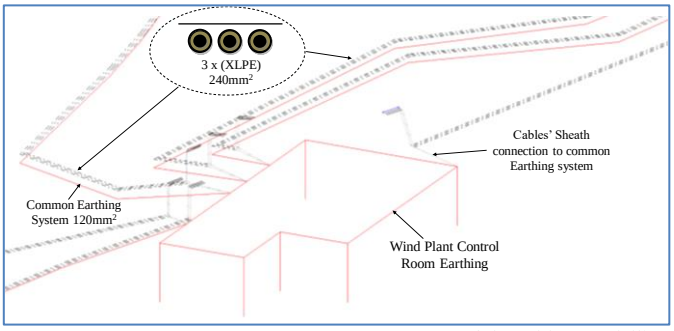

Fig. 5. Simulation Model Showing the Design Detail of the cables' modelling

1) Further Description of Input Data

This subsection provides some further description of the input parameters employed in the EMI simulation model that is shown in Fig. 3. To this objective, Table III shows the characteristics of the pipeline model. It is noted that the pipeline has been modelled for 28km. This is because the pipeline is terminated with insulating joints at the 0th km and 28th km. Moreover, the extensive modelling of the pipeline's routing ensures that the effective resistance to earth of the pipeline as well as its longitudinal impedance is taken into account. This allows for the effects of short-term EMI, at remote locations, to be accurately examined.

TABLE III
CHARACTERISTICS OF BURIED NATURAL GAS PIPELINE

Pipeline wall resistivity (relative to annealed copper)	20
Pipeline wall permeability (relative to free space):	250
Pipeline coating resistivity	10^8 Ωm
Coating thickness	0.0015m
Internal Radius	0.2465 m
Outer Radius	0.254 m
Buried Depth (upper edge)	1.10 m

Table IV illustrates the characteristics of the MV cables used in the EMI model (Fig. 3). The cables were modelled as three separated concentric type cables laid in a flat or trefoil formation.

TABLE IV
CHARACTERISTICS OF BURIED POWER CABLES

Wind Turbines Cables (240mm²) Ampacity (in ground 20ºC): 417A Buried Depth: 1 m				
	Conductor Properties		**Insulation Properties**	
	Core	Sheath	Thickness (mm)	5.5
Inner Radius (m)	0	0.0151	Resistivity (Ωm)	1E+16
Outer Radius (m)	0.0096	0.0179	Relative Permittivity (ε_r)	2.3
Resistivity (Ωm)	2.65 x 10^{-8}	1		
Wind Turbines Cables (630mm²) Ampacity (in ground 20ºC): 675 A Buried Depth: 1 m				
	Conductor Properties		**Insulation Properties**	
	Core	Sheath	Thickness (mm)	6.7
Inner Radius (m)	0	0.02086	Resistivity (Ωm)	1E+16
Outer Radius (m)	0.01416	0.0223	Relative Permittivity (ε_r)	2.3
Resistivity (Ωm)	2.65 x 10^{-8}	1		

Moreover, Figure 6 illustrates the variation of soil resistivity values in the right of way of the 28km section of the gas pipeline. These values were taken under the standard Wenner method [14], and they account for the worst seasonal effects (i.e. dry soil conditions) that apply along the 28km routing. It should be noted that the Wind Park's physical location is very close to the pipeline's routing between the 20th and the 23rd km (see Fig. 3). To this extent, the soil resistivity model used in the simulation, reflects merely on the measurements that had been obtained near 20th and the 23rd km. In particular, a two layer soil resistivity model has been used as follows: Top Layer 741 Ωm (2m) / Lower Layer 1000 Ωm (Infinite Depth).

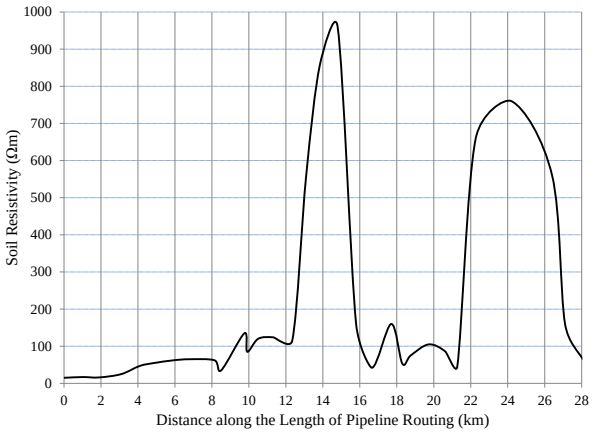

Fig. 6. Soil Resistivity Measurements along the Length of Pipeline

III. ANALYSIS AND DISCUSSION

A. Short-circuit analysis on Wind Park Model (DIgSILENT Power Factory)

The short-circuit analysis of the electrical circuit associated with the Wind Park's electrical topology (Fig. 2), has been exclusively performed in the DIgSILENT software. This supports calculation methods based on the superposition method (also known as the Complete Method) [15]. Briefly, this method embraces the required algorithms and precision for determining realistic short-circuit currents, without considering the simplifying assumptions prescribed in IEC 60909-0:2016 [16]. In this paper the short-circuit analysis pertains merely to single-phase to ground faults. These faults have been simulated at three different locations along the main 20kV XLPE cable (6.2km in length) that connects the control room (C/R) to the MV/HV substation (S/S). In all three fault-scenarios, i.e. (a) near the CR, (b) at the middle of the MV cable and (c) close to the S/S, the ground fault has been simulated on the phase conductor that physically lies closer to the buried gas pipeline. In the interest of space, only the simulation output pertaining to a ground fault - occurring at the middle of the line (50%) between the C/R and the HV-MV S/S – is displayed in Fig.7. However, a summary of the r.m.s results obtained for all three fault scenarios are given in Table V. The results pertain to the total ground fault current as well as the corresponding contribution from the Wind Park (WP) and the HV-MV S/S.

TABLE V
FAULT CURRENT CONTRIBUTIONS FOR SINGLE-PHASE TO GROUND FAULTS (FAULT ON PHASE A)

Fault Location	**Total Fault Current (kA rms)**	**Contribution from S/S (kA rms)**	**Contribution from C/R (kA rms)**
@2% of Line	I_A =4.05∟100.78 º I_B = 0 I_C = 0	I_A = 3.46 ∟ -87 º I_B = 0.19 ∟ -12.4 º I_C = 0.92 ∟ -63.79 º	I_A = 0.78 ∟ -42.28 º I_B = 0.19 ∟ 168.01 º I_C = 0.92 ∟ 116.51 º
@50% of	I_A = 5.15∟98.43 º	I_A = 4.53 ∟ -87.53 º	I_A = 0.8 ∟ -45.75 º

Line	$I_B = 0$ $I_C = 0$	$I_B = 0.25 \angle -19.11^\circ$ $I_C = 0.95 \angle -64.76^\circ$	$I_B = 0.25 \angle 161.2^\circ$ $I_C = 0.95 \angle 115.53^\circ$
@98% of Line	$I_A = 7.16 \angle 94.83^\circ$ $I_B = 0$ $I_C = 0$	$I_A = 6.46 \angle -89.36^\circ$ $I_B = 0.37 \angle -30.99^\circ$ $I_C = 1.03 \angle -66.48^\circ$	$I_A = 0.86 \angle -51.79^\circ$ $I_B = 0.38 \angle 149.07^\circ$ $I_C = 1.03 \angle 113.78^\circ$

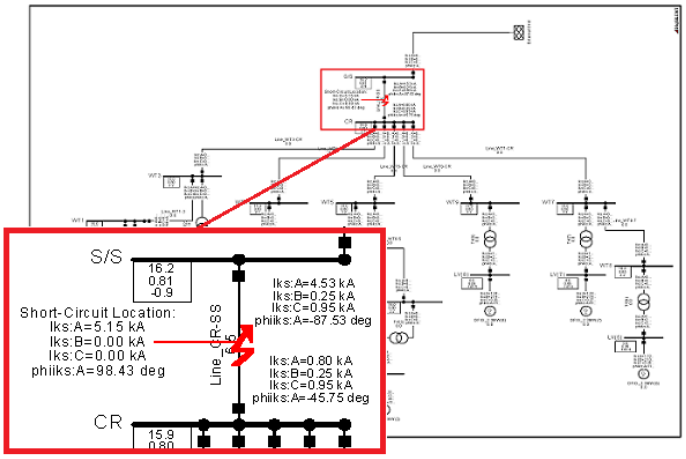

Fig. 7. RMS Fault Analysis for Single-Phase to Ground Fault at the middle of the line (50%)

B. *Spatial EMI analysis on the Buried GAS Pipeline (CDEGS)*

The short-term EMI analysis pertains to the developed model and its associated parameters (See Section II - *C*) that describe the gas pipeline as well the Wind Park's earthing systems and the associated MV power cables.

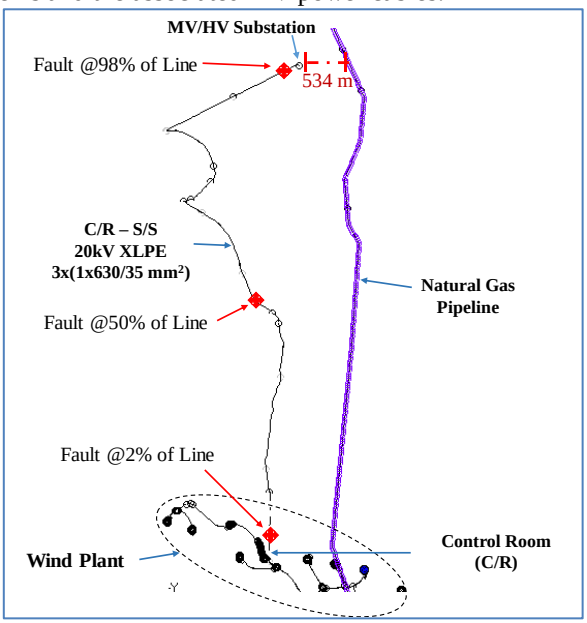

Fig. 8. EMI Model for Simulating Fault Conditions

The model, showing the exact topological arrangement of the systems as well as the locations of the fault scenarios simulated, is presented in Fig. 8. The solution is thus executed within the MultiFields tool of the CDEGS software [13].

1) *Energization of Simulation Model*

The energization of the model in Fig. 8, relies on the short-circuit analysis described above (subsection *A*). In particular, the energization of the model is achieved by the use of *current energization sources* at each terminal of the wind park's - MV cables' connections. That is, for each single-phase to ground fault scenario, the corresponding current flow (e.g. the results in Table V) in all phases/cables - associated with the WP, are utilized. It should be noted, to this extent, that during fault conditions, currents may flow in all three phases, with the maximum current flowing in the faulted phase. Thus, the total net fault flowing to the corresponding fault location, from both sides, should account for the influence of all three phases. In our analysis, this is ensured by virtue of the accurate short-circuit fault calculations performed by the DIgSILENT model that are subsequently interfaced with the EMI model shown in Fig. 8.

2) *Single-Phase to Ground Fault Modelling in Cables' Circuitry*

Within the software used, a single-phase to ground fault is modelled by creating a connection between the cable's core and the sheath, at the location of the fault. Thus, the fault current flows through the sheath and it subsequently discharges where the sheaths are bonded. Thus, the conductive coupling may become significant in places where a large fault current is injected into the earth in areas close to the pipeline[1]. However, the sheath's current may offer some cancellation effect on the induced voltage of the pipeline, owing to the fact that it flows in the opposite direction than the core currents.

3) *Simulation Results (Spatial) and Discussion*

Figure 9 illustrates the simulated coating stress voltage (CSV) along the length of the buried pipeline for the three fault scenarios shown in Table V.

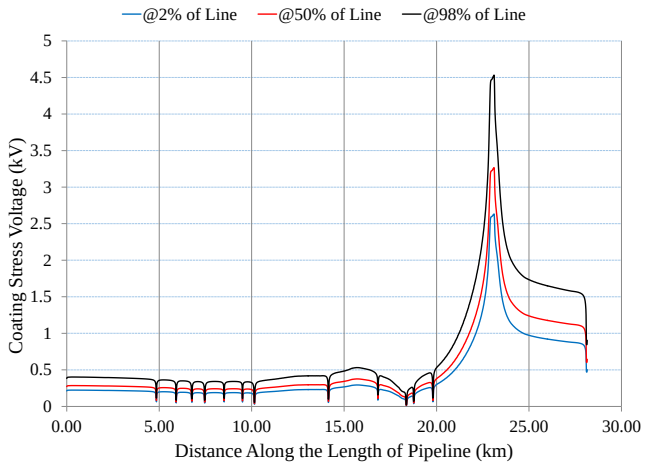

Fig. 9. Coating Stress Voltage along the Length of Pipeline

The results displayed in Fig. 9 pertain to the magnitude (i.e. maximum value) of CSV captured along the entire length of the pipeline (0-28km). Guidance on allowable coating stress voltage varies across references. NACE SP0177-2014 [17] indicates that: "*Limiting the coating stress voltage should be a mitigation objective*." Multiple references offer coating stress

[1] According to EN 50443, the conductive coupling becomes important, under fault conditions, when the interference distance is less than 150 m. Figure 8 illustrates that the actual distance, between the earthing grid of the MV/HV S/S to the nearest pipeline segment, is 534 m.

voltage limits in the range of 2 to 5 kV, depending on the type of coating used, for a short-duration fault [1].

With reference to the results shown in Fig. 9, two important conclusions can be drawn. The first conclusion is that, in this particular case study, the worst short-term EMI result occurs when the single-phase to ground fault occurs at a location that is remote from the Wind Park (i.e. @ 98% of the line length). It is emphasized that this conclusion cannot be generalized; as it is attributed to the topology of the two systems considered (i.e. Wind Park and gas pipeline). The second conclusion is that, in all three fault scenarios the voltage induced on the gas pipeline peaks in the region 21.76 - 23.01km of its routing. The reason for this localized peak can be explained through Fig. 10.

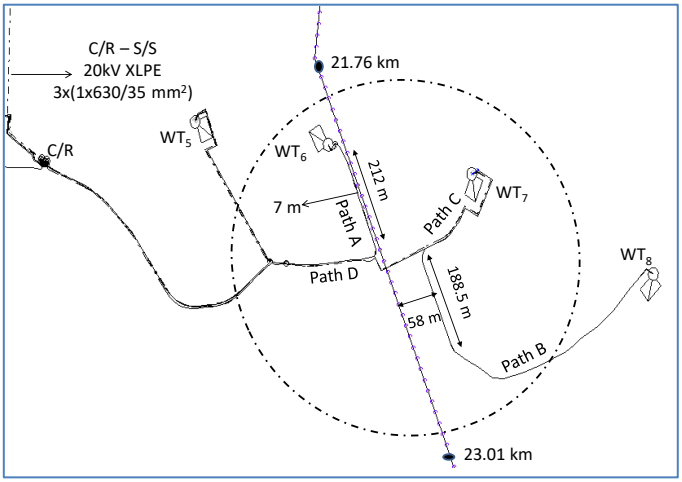

Fig. 10. Topologically accurate detail of the MV cables' routings associated with WT6, WT7 and WT8 with respect to the pipeline routing

This figure shows in a topologically accurate detail that the MV cables' routings associated with WT6, WT7 and WT8 are in close proximity (i.e. parallel for 212m and 188.5m respectively) with the gas pipeline. The distances between the gas pipeline and cables at these parallel routings are 7 with respect to WT6 and 58 m with respect to WT8. To clarify why the EMI result is exacerbated in this particular region, one should examine the fault current flows through the MV cables that are near the 21.76 to 23.01 km pipeline section (see Fig. 10). These current flows are summarized in Table VI for the fault scenario that occurred at @ 98% of the power line's length. In particular, Table VI shows the current flows, in four MV cables' routings, both under steady state and fault operating conditions. The results show that in the event of a single-phase to ground fault, the current flow, through the MV cables of the Wind Park: a) is increased (when compared to the flow under steady state conditions) and b) it is also highly unbalanced. As consequence, the induced voltage along the pipeline is significantly increased in the affected sections.

TABLE VI
FAULT CURRENT CONTRIBUTIONS FOR SINGLE-PHASE TO GROUND FAULTS (FAULT ON PHASE A)

Reference to Fig. 10	Steady State (Balanced)	Single Phase to Ground Fault (Fault on Phase A)
Path A (WT6)	$I_A=I_B=I_C$ = 65. 85 A	I_A = 95.07∟ 128.16 °A I_B = 41.68 ∟ -31.11 °A I_C = 113.79 ∟ -66.27 °A
Path B (WT8)	$I_A=I_B=I_C$ = 67.23 A	I_A = 95.41 ∟ 128.7 °A I_B = 40.8 ∟ -29.63 °A I_C = 114.41 ∟ -66.13 °A
Path C (WT7)	$I_A=I_B=I_C$ = 67.29 A	I_A = 95.59 ∟ 128.59 °A I_B = 41.44 ∟ -29.82 °A I_C = 114.97 ∟ -65.84 °A
Path D (WT7 to CR)	$I_A=I_B=I_C$ = 134.51 A	I_A = 191.06 ∟ 128.64 °A I_B = 81.74 ∟ -29.79 °A I_C = 229.02 ∟ -66.21 °A

4) Mitigation Solution

The limits related to damage of the pipeline systems, under fault conditions, are described in the clauses of EN 50443, as follows: *"The interference voltage (r.m.s. value) between the metallic pipeline system and the earth at any point of the pipeline system, or the interference voltage (r.m.s. value) between any element of the electric/electronic equipment connected between the metallic pipeline and the earth, shall not exceed 2000 V".* It obvious from the above analysis that it is possible for the pipeline's coating performance to be adversely affected by the short-term EMI conditions that have been considered above. In particular, the results in Fig. 9 suggest that in the case of a single-phase to ground fault, the maximum coating stress voltage can be raised to 4.53kV. Thus, the safety limit prescribed in the standard (although conservative) is violated. To mitigate this violation, two additional earthing electrodes are modelled as suggested in Table VII and Fig. 11 respectively.

TABLE VII
SUGGESTED MITIGATION ACTION

Connection @ Pipeline (km)	Length of Electrode (m) / km
22.590 km	50m / 22.540 km -22.590 km
22.630km	100 m/ 22.630km -22.730 km

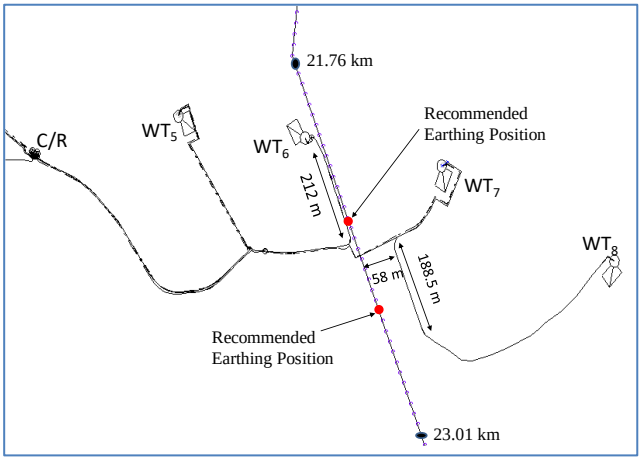

Fig. 11. Recommended Mitigation Solution

The effect of adding these two additional electrodes is shown in Fig. 12. That is, the maximum coating stress voltage under single phase to ground fault conditions limits to about 1.4 kV. Thus, the 2kV threshold limit is met.

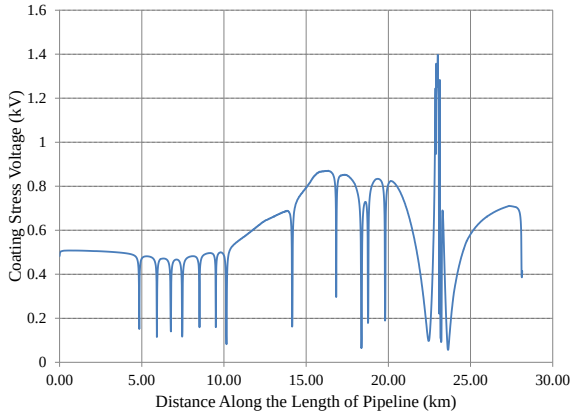

Fig. 12. CSV under the adopted mitigation action

5) Sensitivity Analysis

As previously noted, a single-phase to ground fault is modelled by creating a connection between the cable's core and the sheath, at the location of the fault. Thus, the fault current flows through the sheath and it subsequently discharges where the sheaths are bonded. However, this entails that, at the fault location, there may be no current injected into the earth. The latter suggests that irrespective of the fault location, inductive interference can be the dominant coupling on a collocated buried pipeline. However, it should be kept in mind that the cables' sheaths may be cross-bonded and/or directly bonded to earth at some locations along their routing. Therefore, there may be a degree of current discharge into the earth (i.e. conductive interference). To investigate the latter, we consider a hypothetical sheath bonding configuration for the XLPE cable circuit (6.2 km) that connects the C/R, to the MV/HV substation (S/S). As an illustrative example, the 6.2 km cable circuit is divided into three major sections[2]. Each major section is subdivided into three minor sections of equal length and the sheaths between two-minor sections are cross bonded, as well as earthed (see the layout shown in Fig. 13).

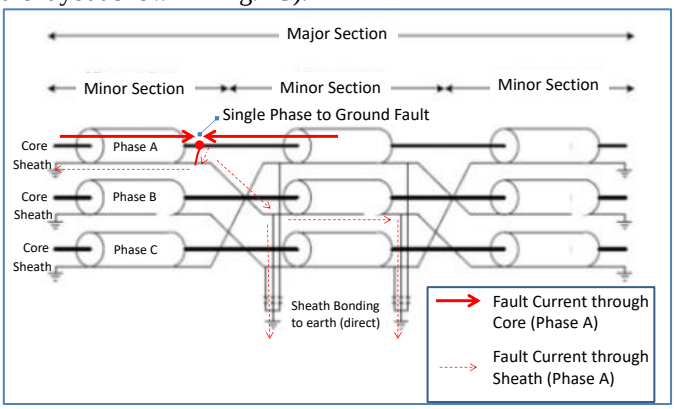

Fig. 13. Example of Sheath Cross Bonding Configuration

To this extent, Fig. 13 illustrates the fault current flows, in the case of a ground fault on Phase A. It is reiterated that this example is merely to facilitate a visual representation of the fact that there may be a degree of fault current discharge into earth depending on the sheath bonding method. The details of this modeling approach (i.e. to account for the sheath bonding method) can be integrated in the simulation model, as shown in Fig. 14.

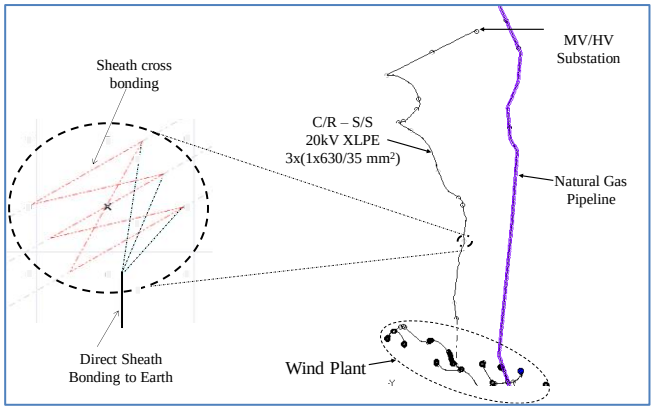

Fig. 14. EMI Simulation Model – Design Detail of Sheath Bonding Method

The simulation results of the above described sensitivity analysis are shown in Fig. 15. In particular, Fig. 15 illustrates a comparison, for the coating stress voltage of the pipeline, under a single-phase to ground fault at 98% of the 6.2km power line. The comparison pertains to the cases where the cables' sheath bonding is considered and respectively omitted, in the simulation process. The first conclusion is that - in terms of the peak coating stress voltage along the pipeline - the results show a 12% reduction (i.e. from 4.53kV to 3.98 kV). However, the change in the coating voltage stress voltage along the entire length of the pipeline can be assessed through Fig. 16. This figure shows the percent variation in the spatial coating stress voltage when the sheath bonding method is taken into account. The results show that the sheath-cross bonding method assumed in this sensitivity analysis, acts to reduce the induced voltage on the pipeline along its entire length.

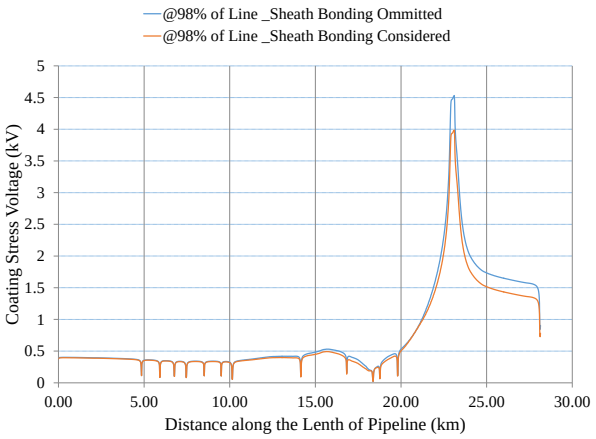

Fig. 15. Comparison of Spatial Coating Stress Under the assumed Sheath Bonding Method

IV. Conclusion

In recent years joint energy corridors are becoming very popular, in an attempt to minimize environmental impacts. A profound example to this aim is the case where underground

[2] In practice the length of the major/minor sections is governed by the allowable induced voltage levels and the geometry of each cable system [18]).

gas pipelines are laid near large renewable energy installations. Through the contents of this paper we aim to highlight that it is possible to have severe EMI events on pipeline systems, due to critical fault events that are associated with these installations. In particular, the impact of critical fault events, associated with Wind Parks' power cables, on the coating stress voltage of a nearby pipeline system has been comprehensively modelled and assessed.

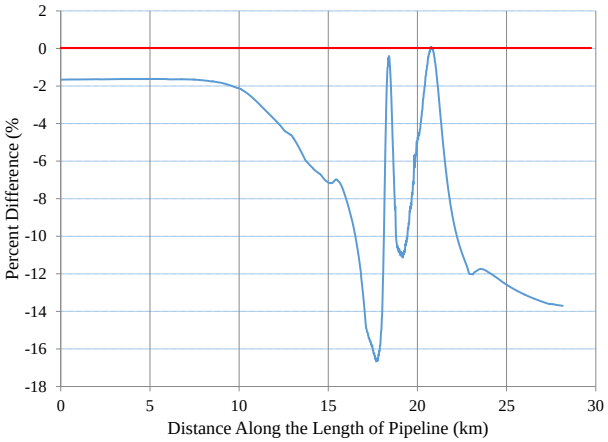

Fig. 16. Percent Variation in Coating Stress Voltage along the Length of Pipeline (when the sheath-bonding is considered)

This was achieved by the concurrent use of two powerful software tools to improve the accuracy of the final evaluation. This is necessary to ensure that the mechanical integrity of the pipeline system would not severely be affected under severe fault events. It is therefore imperative for the EMI mitigation requirements of the pipeline to account for the anticipated power fault conditions of the interference source under study. Where, power cables are involved, it is imperative to include a significant level of complexity in the modelling endeavours. For example the cables' bonding configuration is an important factor that should be definitely taken into consideration. This is to ensure that the impact of the inductive and conductive couplings is concurrently evaluated on the affected pipeline system. The benefit to the practicing engineers and utilities would be that where a mitigation solution is necessary this would neither be over, nor under specified.

REFERENCES

[1] EN 50443:2012 "Effects of electromagnetic interference on pipelines caused by high voltage AC electric traction systems and/or high voltage AC power supply systems", 2012.

[2] Principles and Practices of Electrical Coordination Between Pipelines and Electric Supply Lines, CAN/CSA Standard C22.3 No. 6-13, 2013.

[3] Electrical Hazards on Metallic Pipelines, AS/NZS Standard 4853:2012

[4] ISO 18086:2015, "Corrosion of metals and alloys -- Determination of AC corrosion -- Protection criteria"

[5] C.A. Charalambous, A. Dimitriou, A. Lazari and A. I. Nikolaidis, "Effects of Electromagnetic Interference on Underground Pipelines caused by the Operation of High Voltage A.C. Traction Systems: The Impact of Harmonics", IEEE Transactions on Power Delivery, DOI (identifier) 10.1109/TPWRD.2018.2803080, February 2018.

[6] Wu, X., Zhang, H., & Karady, G. G. (2017). Transient analysis of inductive induced voltage between power line and nearby pipeline. International Journal of Electrical Power and Energy Systems, 84, 47-54. DOI: 10.1016/j.ijepes.2016.04.051.

[7] H. Ding, Y. Zhang, A. M. Gole, D. A. Woodford, M. X. Han and X. N. Xiao, "Analysis of Coupling Effects on Overhead VSC-HVDC Transmission Lines From AC Lines With Shared Right of Way," in IEEE Transactions on Power Delivery, vol. 25, no. 4, pp. 2976-2986, Oct. 2010. doi: 10.1109/TPWRD.2010.2043373.

[8] F. P. Dawalibi and R. D. Southey, "Analysis of electrical interference from power lines to gas pipelines. I. Computation methods," in IEEE Transactions on Power Delivery, vol. 4, no. 3, pp. 1840-1846, Jul 1989. doi: 10.1109/61.32680.

[9] N. Kioupis, , T. Manolis, P. Papadimitriou and C.A. Charalambous, "Failures of insulating joints and spark gaps on the Hellenic Gas Pipeline System - a case study", CEOCOR Conference, 15-18 May 2018, Stratford-upon-Avon, UK.

[10] K. Kopsidas and I. Cotton, "Induced Voltages on Long Aerial and Buried Pipelines Due to Transmission Line Transients," in IEEE Transactions on Power Delivery, vol. 23, no. 3, pp. 1535-1543, July 2008. doi: 10.1109/TPWRD.2007.916234.

[11] G. C. Christoforidis, D. P. Labridis and P. S. Dokopoulos, "Inductive interference on pipelines buried in multilayer soil due to magnetic fields from nearby faulted power lines," in IEEE Transactions on Electromagnetic Compatibility, vol. 47, no. 2, pp. 254-262, May 2005. doi: 10.1109/TEMC.2005.847399.

[12] DIgSILENT GmbH (2017) DIgSILENT Power Factory Version 17 SP3 Gomaringen Germany.

[13] CDEGS Software, Safe Engineering Services & Technologies Ltd Montreal, Quebec, Canada Est. 1978, Version 15.6.

[14] IEEE Guide for Measuring Earth Resistivity, Ground Impedance, and Earth Surface Potentials of a Grounding System, IEEE Std 81™-2012.

[15] J. Duncan Glover Mulukutla S. Sarma Thomas Overbye, "Power System Analysis and Design, Chapter 7: Symmetrical Faults of Power System Analysis and Design" Fifth Edition, ISBN-13: 978-1111425777

[16] IEC 60909-0:2016 "Short-circuit currents in three-phase a.c. systems - Part 0: Calculation of currents".

[17] NACE SP0177-2014 Mitigation of Alternating Current and Lightning Effects on Metallic Structures and Corrosion Control Systems, ISBN: 1-57590-116-1.

[18] CIGRE 283 Technical Brochure, "Special Bonding of High Voltage Power Cables, Working Group B1.18, October 2005.

[19] D. Chrysostomou, A. Dimitriou, N. Kokkinos and C. A. Charalambous, "Short-Term Electromagnetic Interference on a Buried Gas Pipeline Caused by Critical Fault Events of a Wind Park: A Realistic Case Study," 2019 EEEIC / I&CPS Europe, Genova, Italy, 2019, pp. 1-6. doi: 10.1109/EEEIC.2019.8783794

BIOGRAPHIES

Demetris Chrysostomou was born in Nicosia, Cyprus in 1994. He received a first class degree in Electrical Engineering (Bsc) from the University of Cyprus in June 2018. He is currently with ETH Zurich.

Andreas Dimitriou received a MEng (Hons) degree in Electrical & Computer Engineering in 2013 National Technical of Athens (NTUA). He is a PhD candidate within the Power System Modelling Laboratory that operates under the ECE Department of the University of Cyprus.

Nikolaos D. Kokkinos received the M.Sc and Ph.D. degrees in High Voltage Engineering from UMIST in 2001 and 2004 respectively. He is now the C.E.O of ELEMKO, SA. He is a Chartered Engineer (C.Eng. –IET) and since 2007, he is an active member as an expert in 1) the International standardization committee IEC SC 37A, 2) in the European standardization committee CLC TC 37, and 3) in the European standardization committee CLC SC 9XC.

Charalambos A. Charalambous is an Associate Professor, in the Department of Electrical and Computer Engineering, at the University of Cyprus. He is the founder and director of the Power System Modelling Laboratory. His current research interests include solar applications, DC and AC interference and corrosion evaluations in power system applications, earthing/grounding. He is an expert member of in the standardization committee ISO/TC 67/SC 2/WG 24 "DC stray current".